Supplemental document

1, *Immunohistochemical confirmation that GFP positive cells are GABAergic cells.*

Since it is very important to identify if the recorded neurons are excitatory or inhibitory in the present experiment, we first examined how good GFP expression coincides with immunohistochemical identification of GABA expression. In total, we examined 889 cells that were positive against GABA-antibody in the mouse barrel cortex (postnatal day 16 and 20, n = 2). Of these, 803 cells (90.3 %) were judged to be GFP-positive, too (Supplemental Figure 1). The rest of 86 GABA-immunoreactive cells were not GFP-positive. Conversely, there were no opposite cases; all the GFP-positive cells were GABA-positive (n = 803). Although about 10 % of GABA cells failed to show GFP, the fact that all the GFP-positive cells expressed GABA allowed us to conclude that we could reasonably trust GFP as a marker for the GABA population. To further confirm this, we next examined synaptic responses in the monosynaptically connected pairs. We examined whether GFP positive presynaptic cells produce inhibitory postsynaptic potentials in the postsynaptic cells. In total, we tested 262 putative connections by producing action

potentials in these cells (83 GFP-positive cells and 179 GFP-negative cells) while recording neighboring cells simultaneously. Of these, we could record 48 monosynaptic pairs including 16 inhibitory and 32 excitatory pairs. We found all the IPSPs were elicited by presynaptic GFP-positive cells (n=16); similarly, all the EPSPs were elicited by presynaptic GFP-negative cells (n=32). This is another strong piece of evidence that GFP-positive cells were GABAergic and GFP-negative cells were non-GABAergic. Finally, we examined firing properties in response to depolarizing currents, as have been used to identify cell types such as excitatory or inhibitory in the cortex. All the GFP-negative cells showed larger spike frequency adaptation ratio (SR, mean SR= 0.34 ± 0.15 %, n=19) as is the characteristic of regular spiking excitatory neurons. In contrast, GFP-positive cells showed either no or less spike adaptation, as are the characteristics of fast spiking (FS), or regular spiking non pyramidal (RSNP) cells, respectively. This resulted in that the SR in the GFP-positive cells (0.68 ± 0.17 %, n=13) was larger than that of GFP-negative cells. The difference between the SRs for GFP positive and negative cells was significant ($p<0.01$, Student's *t*-test). From these experiments, we could reliably trust the GFP as a marker for GABAergic neurons in the present experiments.

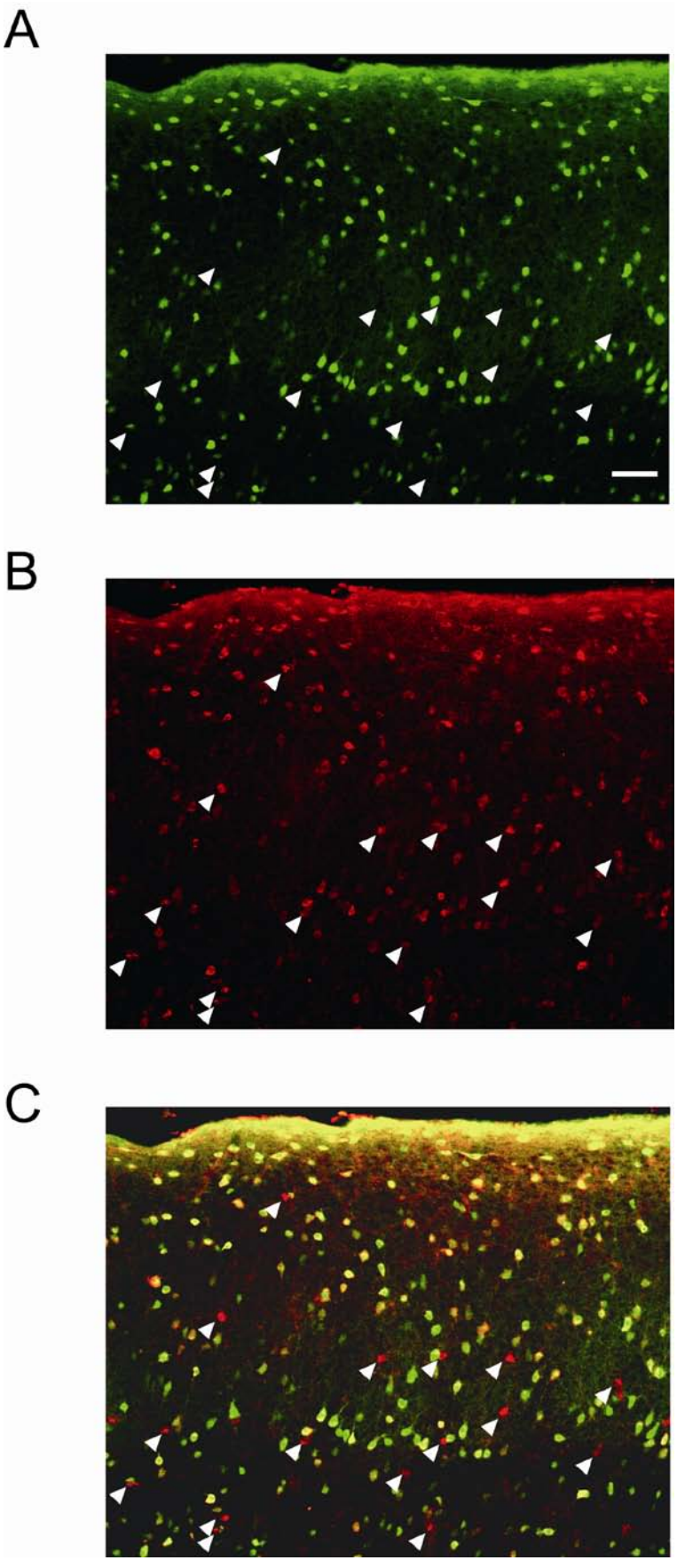
A
B
C

Figure 1

A, Fluorescent photomicrograph of GFP-positive cells. B, immunohistochemical staining using antibody against GABA. C, Overlay of A and B. Scale in A: 100 μm. White arrowheads indicate cells that were positive for GABA staining but negative for GFP, thus appeared red in C.

Methods

Immunohistochemistry

Mouse pups (P16 and P20) were anesthetized deeply with Ethrane (0.9 ml/kg body weight; Abbott Lab, Abbott, IL) and decapitated. The brains were removed, cut into a thalamocortical block (about 10 mm thickness) then fixed for 2 overnights in 2 % paraformaldehyde (PFA) in phosphate-buffered solution (PB 0.2 M) followed by immersion in 30 % sucrose for cryoprotection. The brains were mounted in tissue-tek (Mikes, Elkhart, IN) and made frozen rapidly on dry ice. Thalamocortical blocks were sectioned at a thickness of 40 μm on a cryostat (Leica, Wetzlar, Germany) and mounted on glass slides pre-coated with

Vecta-Bond (Vector Laboratories). The sections were washed in Tris buffered saline (TBS) containing 30 mM Tris-HCl (pH 7.4), 150 mM NaCl and 0.1 % Tween 20, incubated in blocking solution (4 % normal goat serum and 1 % bovine serum albumin in TBS) for 90 min at room temperature and then incubated for 2 overnights at 4 °C with the primary antibody against GABA developed in rabbit (Sigma) at the dilution of 1:1000. After rinsing with TBS, the sections were incubated for 2 h at room temperature with a secondary antibody against rabbit IgG conjugated with Cy-5.

2. *In vivo recording of whisker responses from developing barrel cortex*

Layer specific temporal features of whisker responses in L4 and L2/3

By recording neuronal activities in response to whisker deflection we tested whether principal whisker stimulation would cause activation of L4 and L2/3 cells in this temporal order. We performed simultaneous recording using a single-shaft electrode with 16 vertically aligned probes from cells in L2/3 through L5. As shown in Supplemental Figure 2, at P23 all neurons in the middle depth (channels 7-10), which were later found to be located within L4 by histological

examination, had sharp transient responses to whisker deflection with shorter onset latencies (9.4 ± 0.2 ms) than cells in other layers (13.4 ± 1.5 ms; $P = 0.008$, one-tailed unpaired *t*-test). This is consistent with previous reports (Brumberg et al., 1999; Celikel et al., 2004). Three representative peristimulus time histograms (PSTHs), one from L4 and the others from L2/3 clearly demonstrate that the L4 cells feature fast onsets and narrow response duration, whereas the L2/3 cells feature slower onsets and longer response durations (Brumberg et al., 1999). Although there is an overlap, the “pre” (L4) leading “post” (L2/3) sequence is generally preserved (Celikel et al., 2004). Next, we asked how such characteristics of whisker responses develop with age. Is the change parallel with the establishment of preceding activation of fast feedforward GABA cells? To answer these questions, we performed similar experiments in developing animals.

Developmental changes in whisker responses

At P8, the response time courses looked totally different from those at P23 in all recordings (Supplemental Figure 3), in that the off-responses were stronger than the on-responses as consistent with a previous report (Borgdorff et al., 2007),

and the onset latencies and response durations were extremely longer (89.3 ± 12.4 ms and 112.3 ± 26.8 ms, respectively, n = 6). Importantly, we found no sign of suppression in any cells. This is consistent with the recent finding that GABA produces an excitatory response until the end of the first postnatal week in barrel cortex (Daw et al., 2007). At P11, as shown in Supplemental Figure 4, both onset latencies and response durations were greatly shortened across the layers, although they were still substantially longer than those at P23 (Supplemental Figure 2), and the suppression in L4 was not as complete as at P23. We analyzed quantitatively the developmental changes in time courses of responses at each depth in the cortex by focusing on onset latency and response duration throughout development. The result is summarized in Supplemental Figure 5. At a glance, onset latencies became increasingly shorter during development across the layers. Such changes at layer 4 are clearly seen in the graph (Supplemental Figure 5C), where onset latencies at layer 4 are summarized from P8 to P23. The graph shows a sudden decrease in onset latency between P8 and P11, which is reminiscent of the development of thalamocortical latency (Figure 6A). This would suggest that acceleration of conduction velocity and/or improvement of synaptic transmission take place at various stages from receptor

cells at the whiskers all the way to cortical cells in layer 4. If disynaptic suppression was effectively exerted on L2/3 cells prior to disynaptic excitation as we discussed earlier, onset latency in L2/3 would be delayed. This would be reflected as a monotonic increase in the onset latency as the distance from L4 increase. This is exactly what we see in the graph (Supplemental Figure 5A), where onset latency was plotted as a function of depth (probe number from L4). The graphs showed a monotonic increase with depth from L4 to L2/3 (probe # 0 to negative number on the abscissa) only after P14; thus, the more distant from L4 (probe # 0), the longer the latency, with the shortest latency occurring at L4. Similarly, the response durations also became increasingly shorter during development, thus, the graphs decrease with age (Supplemental Figure 5B). If feedforward inhibition successively curtailed the L4 cell activities (Kyriazi et al., 1998), the response duration of L4 cells would become increasingly shorter. This is clearly seen in Supplemental Figure 5D, in which response duration of cells at L4 is plotted during development. The largest decrease was again seen between P8 and P11, which probably reflects the conversion of GABA response from excitatory to inhibitory (Ben-Ari et al., 1989; Ben-Ari, 2002; Owens and Kriegstein, 2002). It is not until the end of the 1st postnatal week that GABA

receptor activation produces hyperpolarization at thalamocortical synapses (Daw et al., 2007). The second decrease occurred between P11 and P13, which would reflect the completion of the precedent activation of GABA cells from thalamus. Thus, the response duration at P11 is significantly different from that at P13 and P23, after which, no significant decrease was noted. Response durations of cells in layers other than L4 are unrelated to feedforward inhibition by thalamically activated GABA cells, making L4 lowest value in the response versus depth curve (Supplemental Figure 5B). Such shaping of the curve is also completed only after P14, which supports our findings. Altogether, development of the temporal features of whisker-evoked responses in the barrel cortex proceeded in close accordance with development of thalamocortical conduction to inhibitory neurons. These results suggest that maturation of thalamocortical transmission to feedforward GABAergic neurons underlies the development of temporal response properties and spike sequences in the cortical cells.

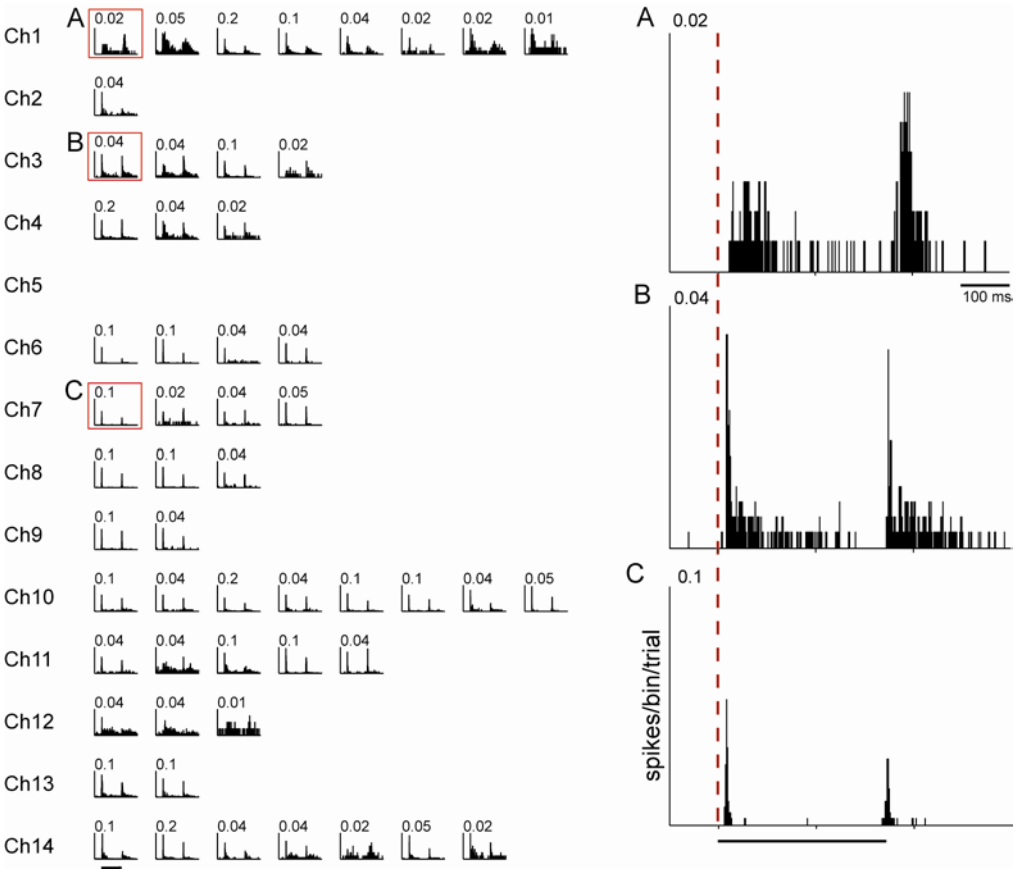

Figure 2

Layer-specific characteristics of peristimulus time histograms (PSTHs) observed in simultaneously recorded neural activities elicited by principle whisker stimulation from a rat at P23. Whisker responses were recorded from an electrode having 16 vertically aligned probes that was inserted perpendicularly to the pial surface covering layer 2/3 to layer 5. PSTHs derived from the same probes are illustrated in the same row. Three neighboring probes were used to identify the location of the recorded cells, thus 16 probes could identify 14

depths. Three examples (A, B, C) from each group, outlined in red, are shown on the right with expanded time scales. From histological reconstruction, Ch6 to Ch10 were located in L4. A red dotted line indicates the onset of whisker stimulation. Numbers on the ordinates represent spikes/bin/trial. Timing of whisker stimulation is shown below the expanded PSTHs.

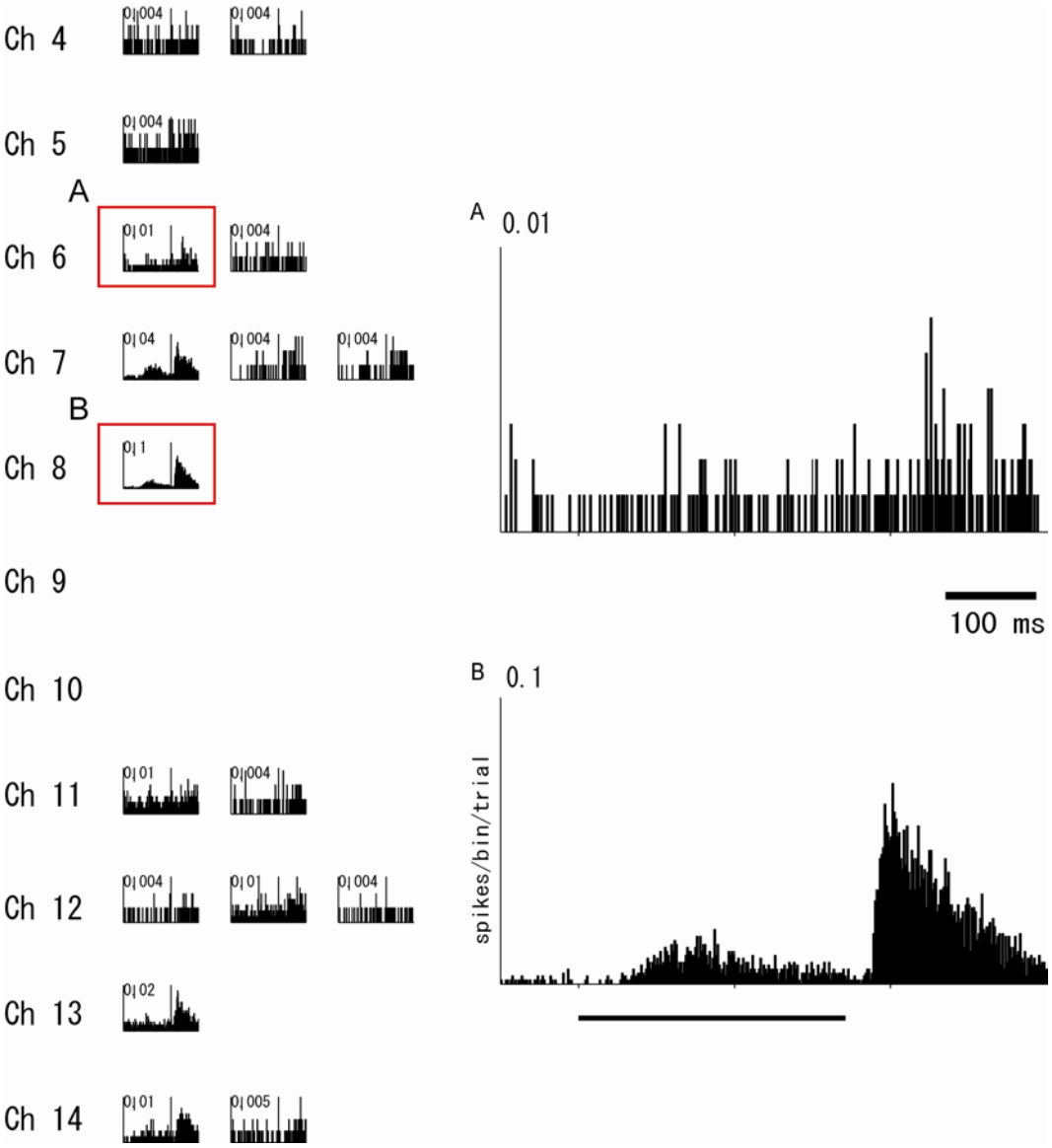

Figure 3

Whisker responses from an 8-day-old rat recorded from multiple depth simultaneously using 16 probes as in Supplemental Figure 2. From histological reconstruction, Ch7 to 10 were located in layer 4. Two PSTHs from layer 4 and layer 3 (red squared) labeled (B) and (A) are shown expanded on the right. Numbers on the Y-axes indicate spikes/bin/trial.

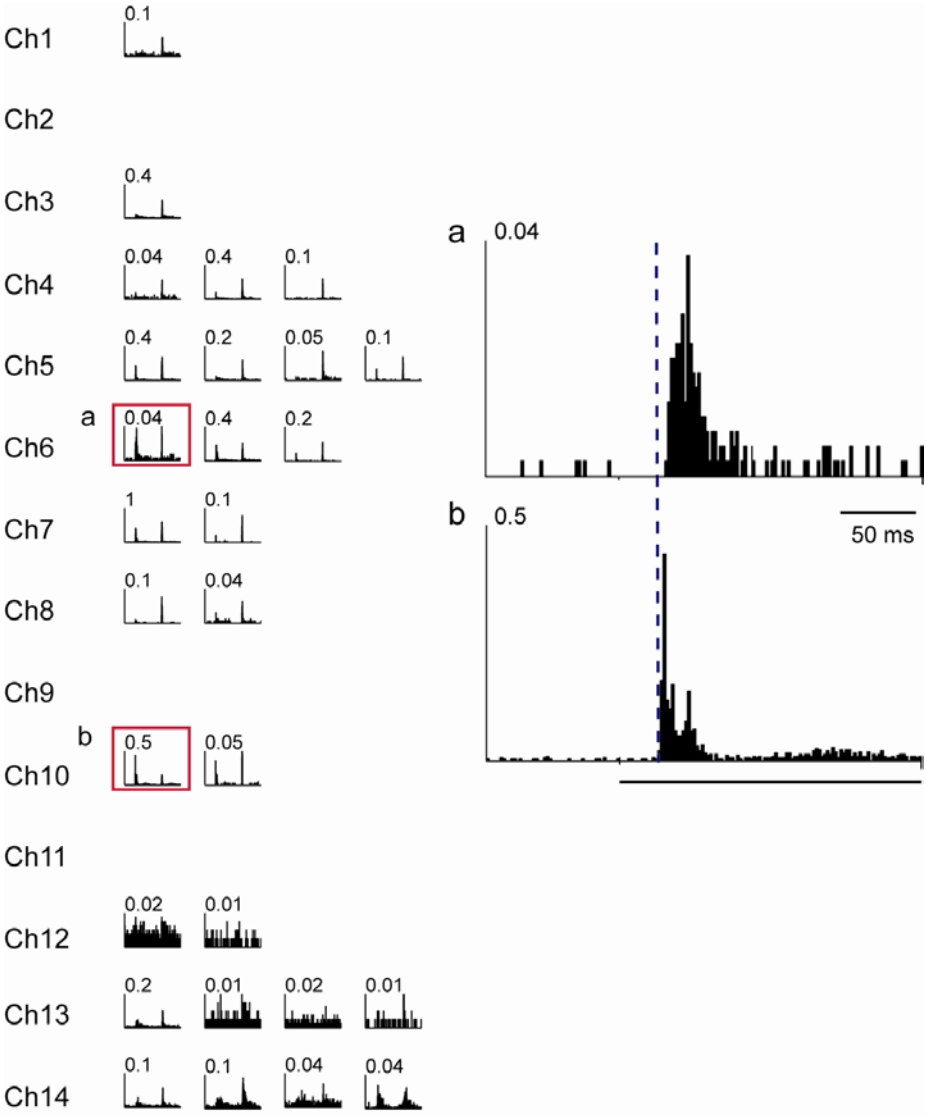

Figure 4

Layer specific characteristics of PSTHs from a P11 rat.

Whisker responses recorded from multiple cells in a P11 rat, similar to those shown in Supplemental Figure 2 and 3. From histological reconstruction, Ch7 to 11 were located in layer 4. Two PSTHs, one from L4 (B) and L2/3 (A) are shown to the right, in an expanded form to include only the on-responses. Numbers on

the Y-axes indicate spikes/bin/trial. Vertical dotted line indicates the onset of response in L4, demonstrating the delayed onset in L2/3 response.

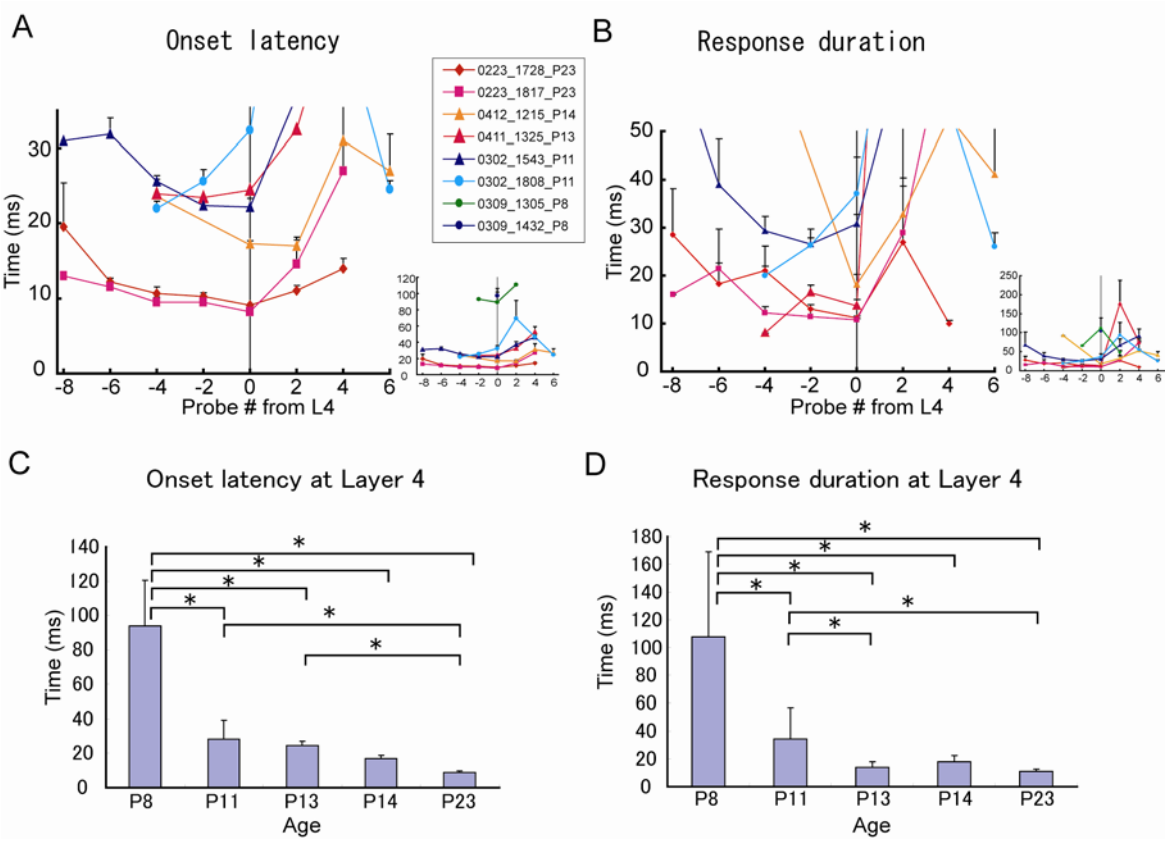

Figure 5

Onset latencies (A) and durations (B) of responses (mean ± SD) are plotted against the distances from layer 4 (Probe # at L4 was designated as 0) as represented by the probe number. Numbers with negative sign correspond to shallower layers (L2/3), and positive signs correspond to deeper layers (L5 and

L6). Simultaneously recorded responses in the same penetrations are connected by lines. Data from eight penetrations from five rats are presented. Each point represents the average from 2 adjacent probes, except for those probes designated for L4. In L4, average was calculated from all the probes found in L4. Expanded onset latency (0-35 ms) and response duration (0-50 ms) are shown, and to the right whole graphs are shown as insets. C, D, Developmental changes in the onset latency (C) or response duration (D) from cells at layer 4 are extracted from A and B, respectively, and plotted against age. Asterisks indicate significant differences among the groups by Post-hoc test ($P<0.05$, Fisher's protected Least Significant Difference).

Methods

In vivo preparation

Sprague-Dawley rats aged 8, 11, 13, 14 and 23 days (5 rats in total) were used. Under deep anesthesia with urethane (1.5 g/kg, i.p.), rats were fixed to a custom-made stereotaxic apparatus. Heart rate and body temperature were continuously monitored during experiments and the latter was maintained at 37 ± 0.1°C. The depth of anesthesia was consistently checked by light pinches

applied to the tail, and when animals responded by an increase of respiration and/or heart rates, additional doses (0.3-0.8 g/kg, i.p.) were given. After administrating local anesthesia xylocaine (~1 ml, subcutaneous), craniotomy was performed over the right S1 area, and the dura was removed.

In vivo multi-electrode recording and whisker stimulation

A linear array of 16 recording probes spaced 50 μm apart (NeuroNexus, MI, USA) was placed vertically to cortical surface. All the recordings were obtained from the right hemisphere. Signals were amplified (x10000), band-pass filtered (0.5–3.0 kHz), and then digitized at 20 kHz. Spike-sorting was performed offline using our own program (Kaneko et al., 1999). For identification of layers, a cathodal current (5–10 μA x 10 s) was passed at 2 of the 16 probes at the end of recording. After the experiments, rats were deeply anesthetized and transcardially perfused with 4% paraformaldehyde. Brains were removed and cut into 60–80 μm serial sections for reconstruction of penetrations.

All whiskers except the principle whisker on the left of the face were cut at the base. The principle whisker was cut to 10 mm from the base and held by a wedge of the stimulating probe. We used a piezoelectric bimorph actuator for

controlled ramp-and-hold deflection of the single whisker. Because flexibility of whiskers differed among different ages of animals, we changed the position at which the stimulating probe attached to the whisker from the base depending on the age of rats (2-7 mm) for a reliable deflection. In every experiment, we continuously monitored and recorded movement of the tip of the stimulus probe using a non-contact laser displacement sensor (LK-G85, Keyence, Osaka; 16 bit, 20 kHz). We observed no ringing of our stimulus probe in all experiments. We determined the onset of deflection offline as the timing when the stimulus probe moved 30 μm from its resting position. The timing of deflection offset was defined as the timing when a probe moved 30 μm back toward the resting position from the holding position. The duration between onset and offset of deflection was 330 ms. The tip moved 1.0 mm over 20 ms (mean velocity: 50 mm/s). Inter-stimulus interval was 2 or 10 s.